

A Novel Handheld Bimanual Surgical Robot for Single-Port Laparoscopic Surgery

Zhe Feng

The First Affiliated Hospital of Xi'an Jiaotong University

Dinghui Dong

The First Affiliated Hospital of Xi'an Jiaotong University

Tao Ma

The First Affiliated Hospital of Xi'an Jiaotong University

Yue Wang

The First Affiliated Hospital of Xi'an Jiaotong University

Huan Chen

The First Affiliated Hospital of Xi'an Jiaotong University

Rongqian Wu

The First Affiliated Hospital of Xi'an Jiaotong University

Yi Lv

The First Affiliated Hospital of Xi'an Jiaotong University

HaoYang Zhu (✉ zhycylmeirenji@163.com)

Xi'an Jiaotong University Medical College First Affiliated Hospital <https://orcid.org/0000-0002-2491-0020>

Research

Keywords: single-port laparoscopic surgery, bimanual surgical robot, kinematic analysis, hepatic cyst

Posted Date: August 25th, 2020

DOI: <https://doi.org/10.21203/rs.3.rs-52101/v1>

License:  This work is licensed under a Creative Commons Attribution 4.0 International License.

[Read Full License](#)

23 **Abstract**

24 Background: single-port laparoscopic surgery is a hotspot of minimally invasive
25 surgery, but its promotion is limited because of operational triangulation and
26 instrument conflict. Robot technologies can cleverly solve this dilemma. But most of
27 the surgery robots need high cost and long time to setup and mainly for complex
28 surgery currently. There is no portable single-port laparoscopic robotic surgical
29 instruments suitable for simple abdominal surgery.

30 Result: This paper presents a handheld single-port laparoscopic surgical robot.
31 It consists of two manipulate arms, both of the arms have 2 degrees of freedom, and
32 two more degrees of freedom can be applied by handheld. The left arm has the
33 function of pulling tissue, while the right arm is equipped with a laser fiber, which
34 can be used for tissue cutting and hemostasis with a 980nm diode laser. Kinematics
35 analysis, dynamic simulation, modal analysis and vitro simulation experiments were
36 conducted to verify the feasibility for the handheld single-port laparoscopic robot. The
37 bimanual surgical robot can provide enough workspace, the gripper and laser head
38 have stable working ability, and can successfully complete the fenestration and
39 drainage of hepatic cyst.

40 Conclusion: This bimanual surgical robot has the potential to become a surgical
41 instrument for simple intraperitoneal surgery. It can provide a small, portable and
42 inexpensive surgical robot system.

43 Keywords: single-port laparoscopic surgery; bimanual surgical robot; kinematic
44 analysis; hepatic cyst

45 **Background:**

46 Laparoscopic surgery, also called minimally invasive surgery (MIS). Laparoscopic
47 surgery not only meets the needs of patients in terms of cosmesis but also can reduce
48 postoperative pain and intestinal obstruction time, so that patients can recover faster,
49 stay in hospital for a shorter time, and return to normal activities earlier(1-5). But most
50 laparoscopic procedures usually requires 3-6 small incisions for ports. Given the
51 development of laparoscopic technique, single-port laparoscopic surgery (SPLS)
52 become a new tendency(6-10). SPLS is more difficulty for surgeon to learn and
53 manipulate because surgical instruments frequently encounter motion limitations and
54 clashing due to crowding. The most important thing is that SPLS significantly increases
55 the difficulty of operative site exposure and dissection due to inability of triangular
56 dissection which has been considered a cornerstone of laparoscopic surgery.

57 So, there are some measures to overcome those limitations, including inverse
58 triangulation, pivoting, spreading out dissection, hanging suture, transluminal
59 traction(11). But these measures either change the surgeon's habit or increase the
60 operations step and often results in awkward hand movements in which the surgeon's
61 hands control the opposite end effectors. Furthermore, robot-assisted technology is a
62 new technology to solve that problem(12). Most of these limitations during multiport
63 laparoscopic surgery have been solved with the aid of robotic technology.

64 Robot-assisted technology has increased the distribution of laparoscopic surgery
65 and revolutionized the way of surgery. Surgeons and research teams have developed
66 several types of single-port laparoscopic robots , including Da Vinci SP(13) ,

67 SPIDER(14), QuadPort(15),etc. The parallel use of robotic surgery with single-port
68 platforms, however, appears to counteract technical issues associated with single
69 incision laparoscopic surgery through significant ergonomic improvements, including
70 enhanced instrument triangulation, organ retraction, and camera localization within the
71 surgical field. Robot-assisted single-port laparoscopic surgery system have been used
72 in radical prostatectomies(13, 16), cystectomy(17), mediastinal mass(18), laryngo-
73 pharyngeal cancer(19), head and neck surgery(20). However, most of those are
74 complicated surgery, and these robot-assisted single-port laparoscopic surgery are
75 bulky and have a long learning curve. Besides, the mean time of setup and takedown
76 for Da Vinci is more than 1 hour and laparoscopic surgery is more cost effective than it
77 in cost analysis with an economic model(21), The longer of the setup and takedown,
78 the longer the patient will have to undergo general anesthesia. those disadvantages
79 making them difficult to promote in primary hospitals. So, the current RASPLS is not
80 apply to everyone who needs surgery, especially the poor and the surgery is less
81 complicated.

82 Hepatic cyst is a common benign disease of the liver. Some patients with the
83 increasing of cyst or oppression surrounding tissue can appear some symptoms,
84 including abdominal pain, bloating, liver enlargement, abdominal mass, nausea,
85 vomiting, and loss of appetite. More serious can appear ascites, edema, jaundice,
86 hemorrhagic hepatic cyst and other symptoms(22-24). Today, laparoscopic with two or
87 three ports has been widely used in fenestration and drainage of hepatic cyst(24). We
88 should also pursue a single port laparoscopic to this procedure. But, using the da Vinci®

89 Surgical System is too expensive to extended to everyone.

90 So, we need portable surgery robots that cheap and easy to setup and operate. In
91 this paper, wo present a microsurgical robot for laparoscopic surgery. The device that
92 mounted a 980-nm diode laser(25) on the right arm for incising can be used to operate
93 fenestration and drainage of hepatic cyst under a magnetically anchored camera(26),
94 The feasibility of the equipment was verified through kinematics analysis, dynamic
95 simulation and simulated vitro experiment.

96 **Result:**

97 1. Kinematic analysis

98 The bimanual robot consists of a left arm and a right arm. Both arms have the same
99 range of motion of joints, internal structure and size, so as long as we conduct the
100 kinematic analysis on either of them, we can obtain the kinematic characteristics of the
101 other.

102 1.1 Establishment of connecting rod and connecting rod coordinate system

103 The bimanual robot has four degrees of freedom, namely three degrees of rotation
104 and one degree of movement. In this paper, D-H method is adopted to establish the
105 coordinate system of each link of the robot, as shown in Fig 1. The relationship between
106 adjacent links is represented by four parameters (Table 1), θ -joint Angle, d- link offset,
107 a-link length and α -twist Angle. The two degrees of freedom, θ_1 and d, are
108 generated by the hand. Other two DOF , θ_2 and θ_3 , are generated by the robot itself.

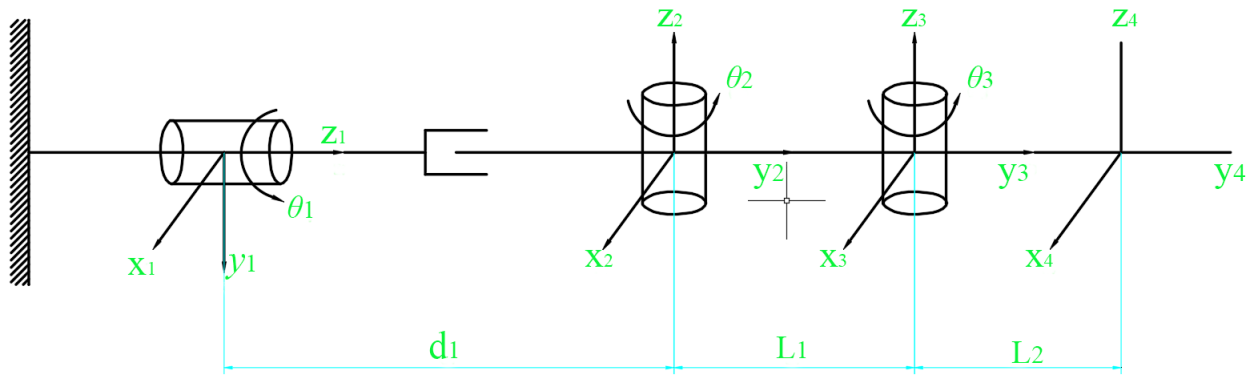


Fig.1 Coordinate system of each link of the robot

109

110

Table 1. Connecting rod parameters and joint variables of left arm of the bimanual robot

adjacent links	Joint rotation angle, θ ($^\circ$)	Twist angle, α ($^\circ$)	Distance d_i , (mm)	Rod length, a (mm)	Range of rotation angle, ($^\circ$)
1	θ_1 (0)	0	d_1 (0~30)	0	$0 \sim -360^\circ$
2	θ_2 (0)	0	0	35	$-45^\circ \sim 45^\circ$
3	θ_3 (0)	0	0	50	$-45^\circ \sim 45^\circ$

112

113 With D-H method, use a 4x4 homogeneous transformation matrix to describe the
 114 spatial relationship between two connecting rods, and allow the coordinate system $\{i\}$
 115 to be coincident with the coordinate system $\{i-1\}$ through rotation and translation.
 116 Therefore, the coordinate transformation matrix of the coordinate system $\{i\}$ in the
 117 coordinate system $\{i-1\}$ is:

118
$${}^{i-1}_i T = Rot(x, \alpha_i) Trans(a_{i-1}, 0, 0) Rot(z, \theta_i) Trans(0, 0, d_i)$$

119 According to the above method and the relevant data in Table 1, it is possible to
 120 establish the equivalent homogeneous transformation matrix of the coordinate system
 121 of the end tool (grippers or laser head) relative to the base coordinate system in turn, so
 122 as to establish the kinematic equation of the bimanual robot. The orientation matrix of
 123 the execution end in the base coordinate system is ($q1$ represents θ_1 , and so on) :

124
$$T1 = \begin{bmatrix} -\sin(q1), & -\cos(q1), & 0, & 0 \\ \cos(q1), & -\sin(q1), & 0, & 0 \\ 0, & 0, & 0, & d1 \\ 0, & 0, & 0, & 1 \end{bmatrix}$$

125
$$T2 = \begin{bmatrix} \cos(q2), & -\sin(q2), & 0, & -L1 * \sin(q2) \\ \sin(q2), & \cos(q2), & 0, & L1 * \cos(q2) \\ 0, & 0, & 1, & 0 \\ 0, & 0, & 0, & 1 \end{bmatrix}$$

126

127
$$T3 = \begin{bmatrix} \cos(q3), & -\sin(q3), & 0, & -L2 * \sin(q3) \\ \sin(q3), & \cos(q3), & 0, & L2 * \cos(q3) \\ 0, & 0, & 1, & 0 \\ 0, & 0, & 0, & 1 \end{bmatrix}$$

128
$$T = T1 * T2 * T3 = \begin{bmatrix} n_x & o_x & a_x & p_x \\ n_y & o_y & a_y & p_y \\ n_z & o_z & a_z & p_z \\ 0 & 0 & 0 & 1 \end{bmatrix}$$

129 $\vec{n}, \vec{o}, \vec{a}, \vec{p}$ are normal vector, direction vector, approach vector and position vector
 130 of the execution end, respectively. The coordinate system of the execution end is in the
 131 same direction as the base coordinate system.

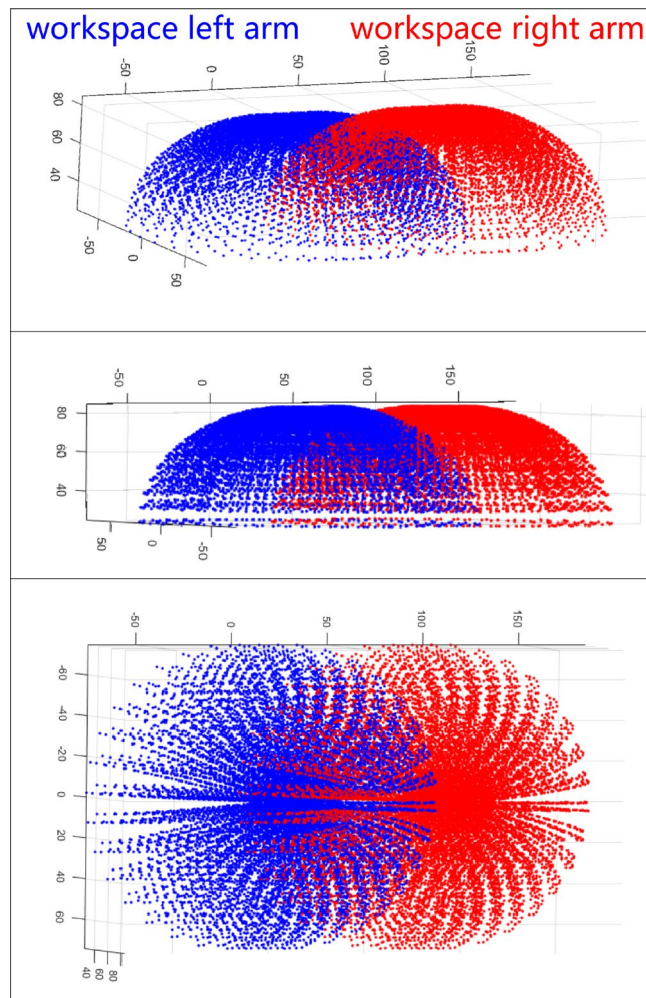
132 1.2 Simulation analysis of the workspace

133 Based on the position and attitude of the coordinate system of the end actuator and
 134 the rotation range of each joint, simulate the workspace by programming in MATLAB

135 with Monte Carlo method, and obtain the 3D point cloud diagram of the whole space.

136 The workspaces of the robot is shown in Fig 2.

137



138

Fig.2 The workspaces of the bimanual robot

139

140 2. Dynamic simulation analysis

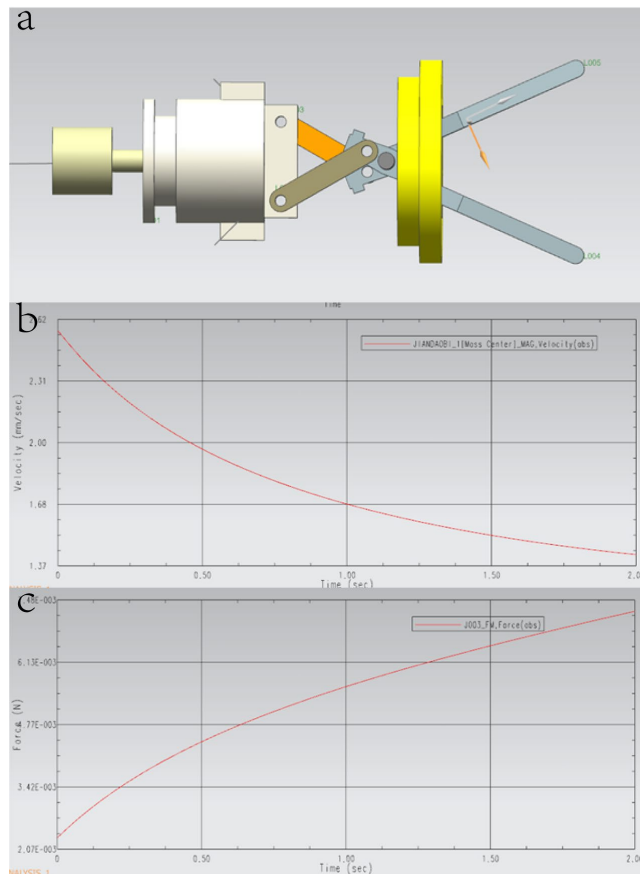
141 The gripper is mainly used to drive the slide by the motor to make a linear motion

142 in the shell, which is finally converted into the stripping action of the actuator end of

143 the rod-mechanism. Obtain the stripping force of the stripper through dynamic

144 simulation analysis, as well as the speed and acceleration curve of the working process.

145 The highest torque of the motor is $900\text{g}\cdot\text{cm}(88.2\text{N}\cdot\text{mm})$. In the operation, the motor
 146 is connected with the slide through inside sleeve with threaded. Parameters are as
 147 follows: thread median diameter $d=7.51\text{mm}$, lead of thread $S=1\text{mm}$, thread angle
 148 $\alpha=30^\circ$. The thrust F generated by the slide is expressed with the following equation:
 149 $F = \frac{2T}{d \times \tan(\gamma + \rho_v)}$, Where, γ -guide stroke angle, $\gamma = \arctan \frac{S}{\pi d}$; ρ_v -equivalent
 150 friction angle, $\rho_v = \arctan \frac{u}{\cos \frac{\alpha}{2}}$; u -friction coefficient, find it to be 0.08 by
 151 looking up the table. Obtain the thrust generated by the slider by substituting the
 152 above parameters into the equation, $F = 175\text{N}$.



153
 154

Fig.3 kinematic simulation analysis

155 Based on the above calculation results, import the model into the UG
 156 simulation module (Fig.3), and establish the dynamic simulation model of the

157 stripper (Fig.3a). the speed and force of gripper changing smoothly in dynamic
158 simulation (Fig.3b, c).

159 3. Modal analysis

160 Upon operation of the bimanual robot, the parts will inevitably produce forced
161 vibration under the action of periodic load. Especially when the excitation frequency of
162 the exciting force is equal to or close to the natural frequency of the parts, the resonance
163 of the structure will occur, resulting in strong vibration noise and structural damage.
164 Modal analysis can evaluate the natural vibration characteristics of mechanical
165 structures. The finite element analysis (FEA) method is a numerical calculation method
166 used to solve various engineering problems. For a continuous system with an actual
167 elastic structure, the kinetic balance equation of the discrete system with n-DOF can be
168 obtained by discretizing it with the FEA, and the finite element calculation equation of
169 the system is:

$$170 \quad [M]\ddot{u} + [C]\dot{u} + [K]u = [F] \quad (1)$$

171 Where, $[M]$ is the mass matrix, $[C]$ 为 is the damping matrix, $[K]$ is the
172 rigidity matrix, \ddot{u} is the acceleration vector, \dot{u} is the acceleration vector, u is the
173 displacement vector, and $[F]$ is the external load matrix.

174 Static analysis refers to analyzing the stress distribution and strain of the
175 structure under the static load. Upon analysis, the quantities related to time t are
176 ignored. So Equation (1) is simplified as:

$$177 \quad [K]u = [F] \quad (2)$$

178 The model of relevant parts of the bimanual robot is the undamped multi-DOF
179 linear vibration system, with its kinematic equation as follows:

$$180 \quad [M]\ddot{u} + [K]u = [0] \quad (3)$$

181 The undamped modal analysis model is a typical eigenvalue problem with its
182 solution form as follows:

$$183 \quad u = u_i \sin(\omega_i t) \quad (i = 1, 2 \dots n) \quad (4)$$

184 By substituting Equation (4) into Equation (3), obtain:

$$185 \quad ([K] - \omega_i^2 [M])u_i = [0] \quad (5)$$

186 The eigenvalue of Equation (5) is ω_i^2 , ω_i is the frequency of the system
187 vibration circle, and the eigenvector u_i corresponding to ω_i is the mode of
188 vibration corresponding to the natural vibration frequency $f = \frac{\omega_i}{2\pi}$.

189 The structure of the left arm is basically the same as that of the right one, and the
190 stability of the laser head is very important during operation because laser head will
191 result in inaccurate positioning due to structural resonance. So, modal analysis of the
192 left arm of bimanual robot and the laser head is carried out in this paper. The results of
193 the right one can be referenced from those of the left bimanual robot. The first six-order
194 modal frequency and the first three-order mode of vibration of each part are obtained.

195 For the ease of calculation, it is assumed that each joint position is fixed through
196 is rigid connection. See Table 2 for the first six-order modal frequencies of the left arm.
197 The resonance frequencies of left arm of bimanual robot range from 65.01 Hz to
198 412.62Hz. The modal analysis of the laser head is carried out. The first six-order modes

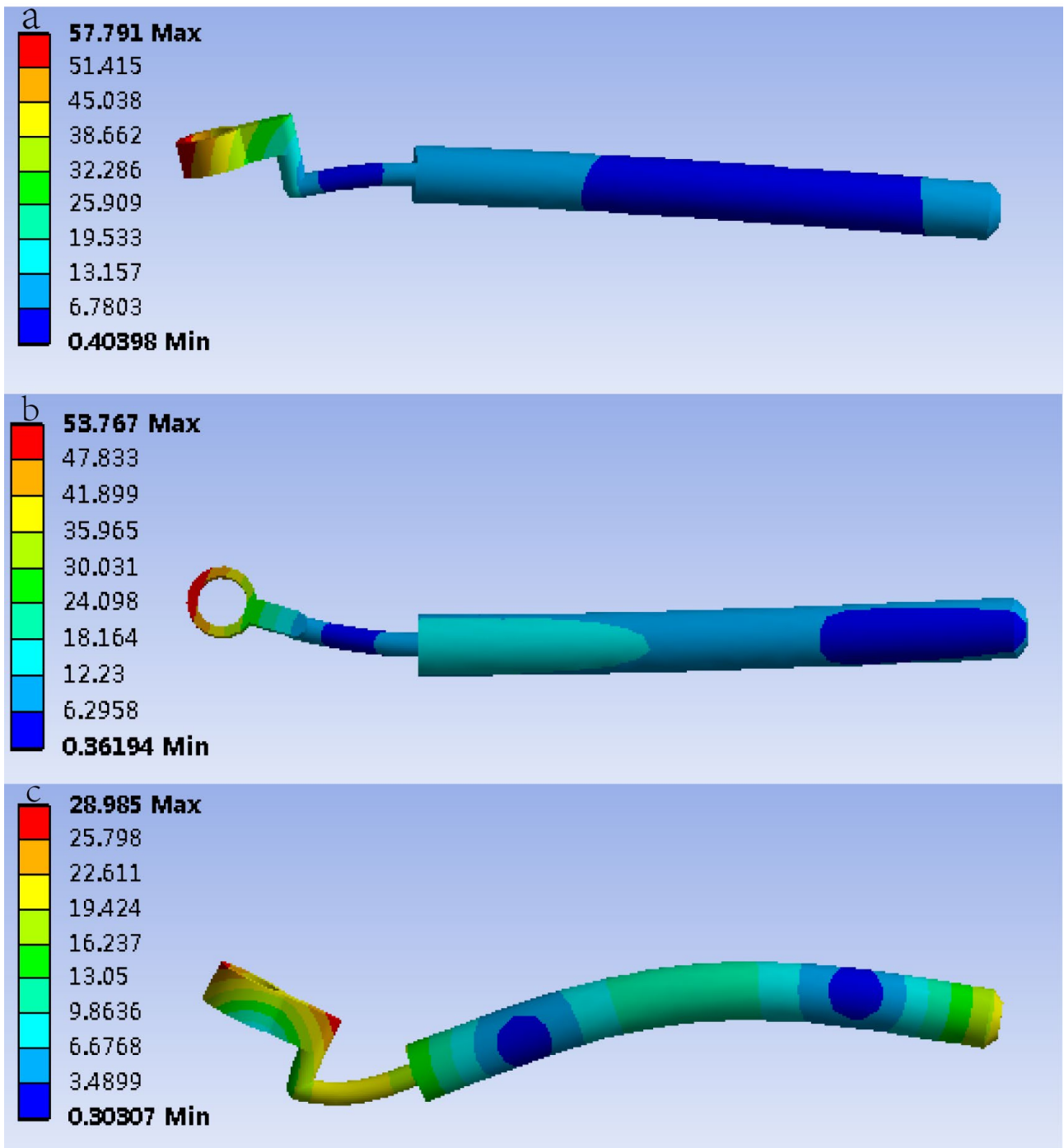
199 of vibration are shown in Table 2. The resonance frequencies of laser head of bimanual
200 robot range from 2851.2 Hz to 15249Hz.

201 Table.2 the first six-order modal frequencies of the bimanual robot

Component	one	two	three	four	five	six
Left arm(Hz)	65.01	71.58	136.89	140.68	366.19	412.62
Laser head(Hz)	2851.2	3104.2	8200.8	8448.1	11137	15249

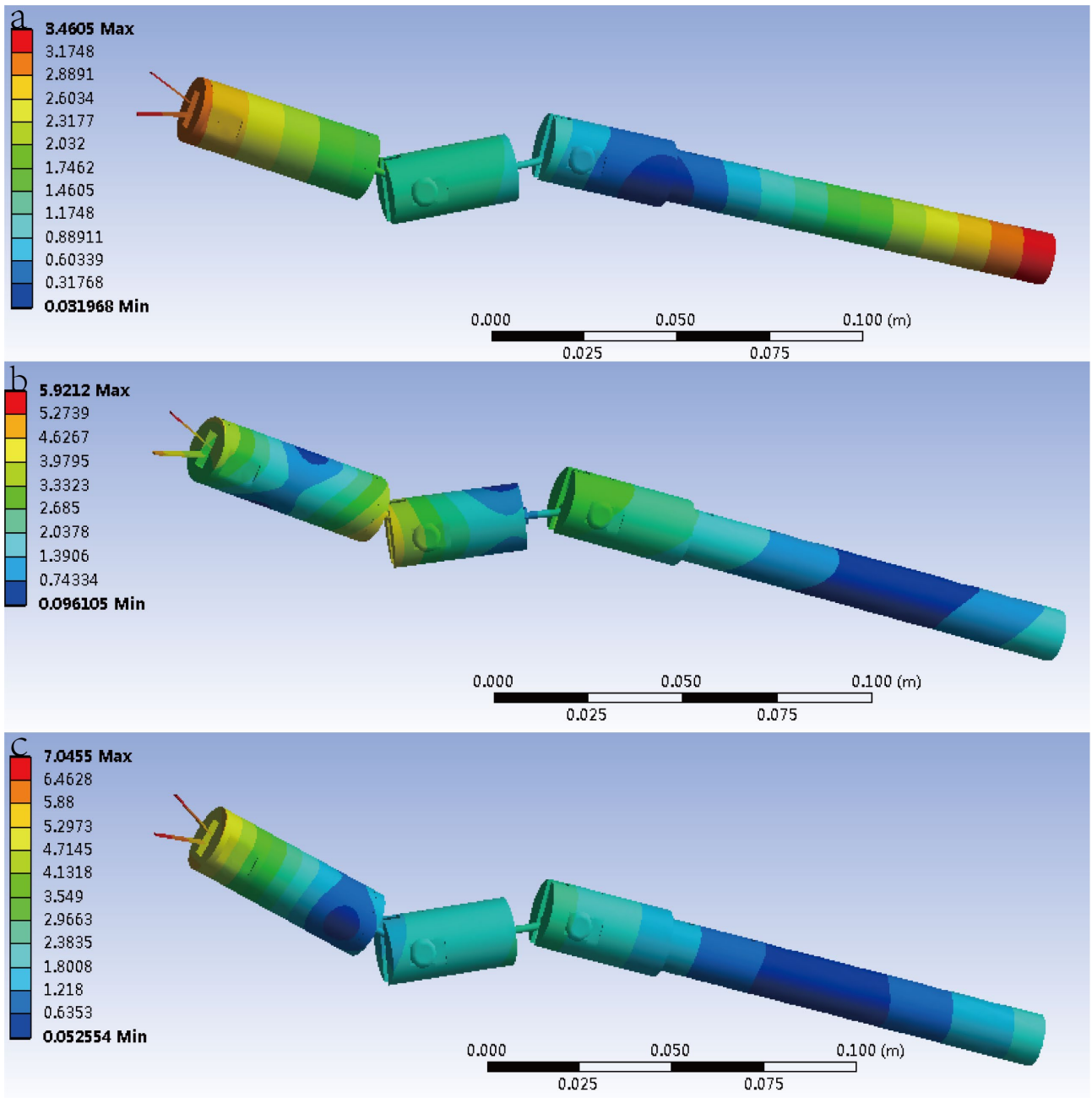
202

203 In order to represent the vibration characteristics of the left bimanual robot at a
204 certain working position in an intuitive manner, select the first three-order modes of
205 vibration of the left arm for calculation, as shown in Fig 4. The frequency values in
206 Table 2 shall not appear in the operation, so the structural resonance will not occur. The
207 first three-order modes of vibration of laser head are shown in Fig 5.



208 Fig.4 Modal analysis of the left arm; a: first-order modal frequencies of the left
 209 bimanual robot; b. second-order modal frequencies of the left bimanual robot; c:
 210 third-order modal frequencies of the left bimanual robot

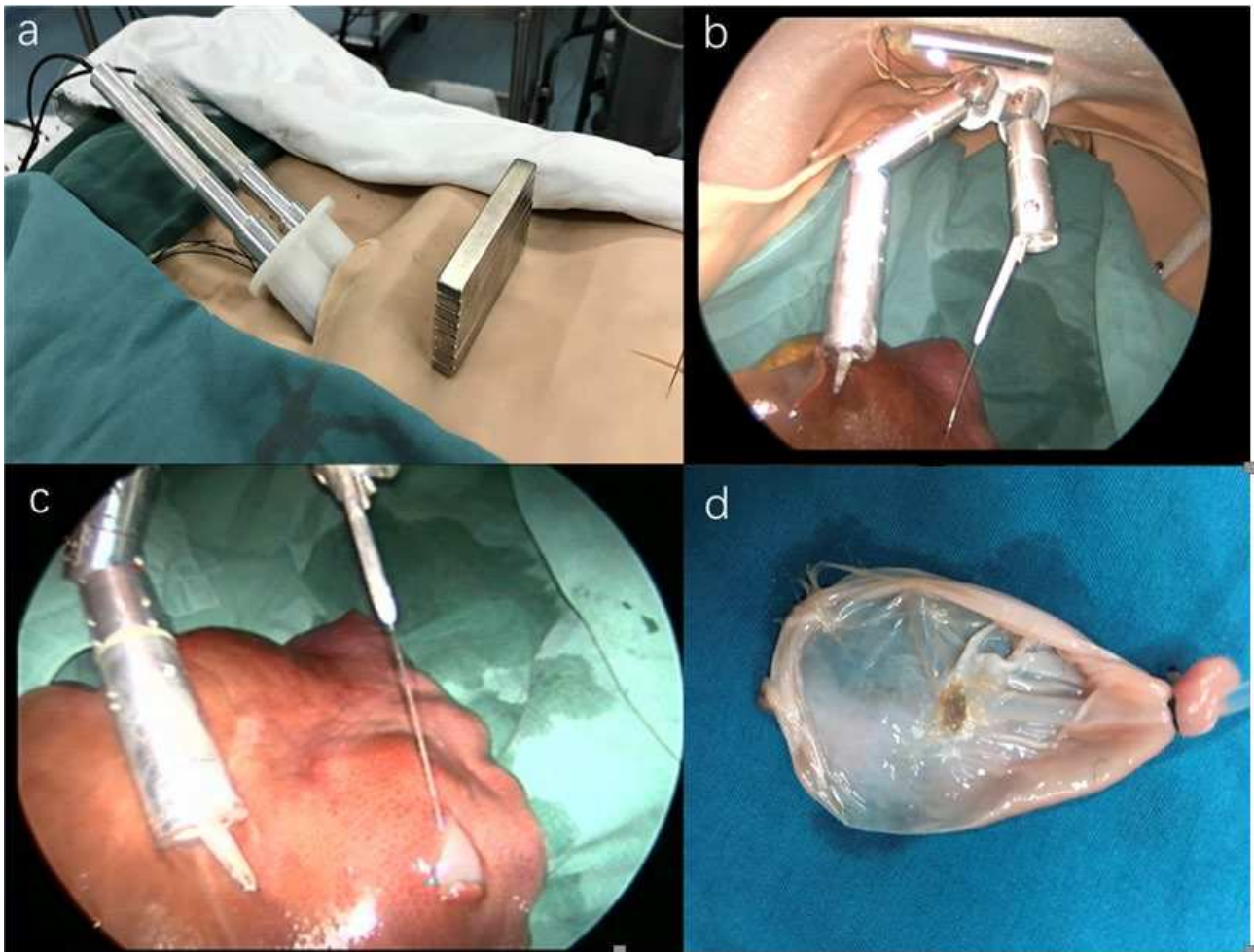
211



212 Fig.5 a: first-order modal frequencies of the laser head; b: second-order modal
 213 frequencies of the laser head; c: third-order modal frequencies of the laser head

214 4. Vitro experiment

215 We conduct the vitro simulation experiment of the bimanual robot in a laboratory
216 platform for fenestration and drainage of hepatic cyst (Fig.6).



217 Fig.6 vitro experiment of fenestration and drainage of hepatic cyst

218 A laparoscopy training platform, called the ex vivo real-liver laparoscopic training
219 system, was used as the bench test in this study. A fresh pork liver was obtained from
220 the slaughterhouse. The swim bladder is tied tightly after filling with water and inserted
221 into a subcapsular to simulate liver cyst. A 40mm high external magnet is used to
222 anchor the mini-magnetically laparoscope. Then the bimanual robot is placed into the
223 abdomen through a 22mm×15mm trocar in the middle abdomen. The umbilical is
224 placed a 10mm traditional endoscopic trocar, which for observing the movement and

225 operation process of the bimanual robot by laparoscope. The left arm grippers the cyst
 226 wall first, and the laser fiber load in right arm can cut the cyst wall. Five cases of
 227 fenestration and drainage of hepatic cyst are performed by bimanual robot. The
 228 completion of the experiment is shown in table 3.

229 Table 3 result of vitro experiment

Number	Success of imbed in abdomen	Instrument interaction	operate fluency	Gripper strength	Operate success	Operate time(min)	Setup time(min)	cause of failure
1	Yes	no	Yes	enough	yes	22	6	-
2	Yes	no	Yes	poor	no	2	7	Laser fiber damage
3	Yes	mild	Yes	enough	yes	21	5	-
4	Yes	no	Yes	enough	yes	20	5	-
5	Yes	no	Yes	enough	yes	20	4	-

230 **Discussion:**

231 Laparoscopic was been used to perform appendectomy and cholecystectomy
 232 earlier(27). Then, the laparoscopic surgery technique has continued to grow quickly.
 233 Laparoscopy was soon applied to abdominal surgery(28)and urology(29) and the
 234 security has been verified(30, 31).Over the last decades, surgeons have been committed

235 to the improvement of laparoscopic technique. Comparing with conventional
236 laparoscopy, single-incision laparoscopic surgery has shown lower pain scores and a
237 shorter hospital stay(32, 33). SPLS has achieved an effective and safe therapeutic effect
238 on both benign disease and cancer(34-37) and reduce the risk of organ injury,
239 hemorrhage, and postoperative adhesions(38, 39). Proponents argued that single-
240 incision laparoscopic surgery will supersede conventional multiport laparoscopy by
241 overcome the shortcoming of conventional multiport laparoscopy, in the same way that
242 laparoscopic surgery superseded the open alternative. But the SPLS not widespread in
243 surgery because the motion limitations and clashing of surgical instruments due to
244 crowding and lack of triangular dissection. With the development of robotics, research
245 team have realized that robotics can effectively solve the problems faced by SPLS. Most
246 robot-assisted MIS systems are equipped with a master–slave teleoperation system for
247 convention multiple ports Laparoscopic surgery. including da Vinci®, MiroSurge, Sofie,
248 Robin Heart, and MicroHand A were developed by leading research teams in the
249 world(40). Growing number of teams are working on convenient single-port
250 laparoscopic robots. The application of single-incision laparoscopic surgery had most
251 commonly been used for cholecystectomy within general surgery. So, there are some
252 team using the Da Vinci Si Surgical System to operate cholecystectomy(41, 42). A
253 team has used Da Vinci SP for a 59 years old woman with chronic calculus cholecystitis
254 to operate cholecystectomy in 89 minutes recently(43). Although the cholecystectomy
255 was completed successfully using the Da Vinci Si Surgical System or Da Vinci SP, such
256 a substantial cost is not suitable to be extended to all patients requiring cholecystectomy.

257 Furthermore, due to Da Vinci System large dimensions, it has a negative impact on the
258 operating room and the setup before a surgical intervention is a very time-consuming
259 process. Besides, most of these surgery robot systems are bulky, expensive, and have a
260 long learning curve, making them difficult to promote in primary hospitals.

261 This paper describes a novel handheld bimanual robot that can be ease of set up
262 and use by a single port of 28mm. The robot carries magnetic anchored camera and
263 980-nm diode laser result in don't need an extra port to set laparoscope and tissue
264 scissors. Each robotic arm was designed with a maximum diameter of 14mm and a total
265 length of 330mm plus the extra DOF provide by hands, resulting in an adequate surgical
266 workspace within the patient's abdomen. The hybrid actuation approach results in a
267 convenient trade-off between the complexity of the robotic structure and the workspace,
268 while still guaranteeing dexterity and telemanipulation capabilities for the surgeon. The
269 major contribution of this work is the operating triangle provided by the robot itself can
270 solve the problem of the interaction of intra-abdominal instruments. This structure
271 avoids spending more time to setup time also. Our bimanual robot takes only four to
272 seven minutes to setup, we argue that in real surgery will still be much less than the
273 current robot setup time. When the robot is not working state, its arms are parallel and
274 it can easily enter the abdomen. The whole structure of the robot adopts rigid connection,
275 can supply for high torque transmission capability and avoid the instability of cable
276 connection.

277 To verify the feasibility of the bimanual robot, three kinds of tests were performed
278 –kinematic analysis, dynamic simulation, modal analysis, and vitro experiment – with

279 each obtaining satisfactory results. Kinematic analysis suggests the robot can provide
280 enough workspace and modal analysis suggests that the robot will not cause additional
281 damage to the target and itself due to resonance. We can find the speed and force of
282 gripper changing smoothly in dynamic simulation. So, the gripper will not cause
283 secondary damage. Although in the in vitro experiment, the failure of the experiment
284 was caused by the damage of the laser fiber, we realize that was not caused by resonance,
285 but by the improper operation. Comparing with the compact single-site robotic surgical
286 system(44), the structure of our robot is simpler and portable, and the incision size for
287 setting the bimanual robot is smaller because the operation of the triangle is forming in
288 abdominal while the triangle outside of abdominal need bigger incision size. With the
289 handheld, surgeons don't need a operate platform(45). This will lead to lower robot
290 manufacturing costs, which in turn will reduce patient costs.

291 The bimanual surgical robot loads a laser knife for incising tissue, it can cut and
292 stop bleeding without contact tissue. The high-frequency electrical surgical knife will
293 generate complex electromagnetic environments that will affect the normal operation
294 of electronic equipment. In serious cases, the function of electronic equipment will be
295 lost or even damaged. And once the electrode breaks down in contact with the patient,
296 it is easy to cause electric burning, burns and fire hazards(46). But, those drawbacks
297 will not occur in laser knife because of the non-contact way and its physical
298 characteristics.

299 However, the strength of the robot is not enough to operate other procedure, further
300 research would need to be made by improving the structure designation(47). Future

301 works will focus on improving system accuracy and more driving force. In addition,
302 we also need to improve the robotics arm execute speed to ensure that the robot can
303 efficiently complete the precise operation during the surgery. At the same time, for the
304 convenience and practical use of surgeons, a good interactive system should be
305 designed, and finally a robot can be operated by one physician. While much work
306 remains to be done, the bimanual robot still achieved the specific design goals. We
307 expect more advanced surgical tasks with in vivo animal models will be performed in
308 the near future.

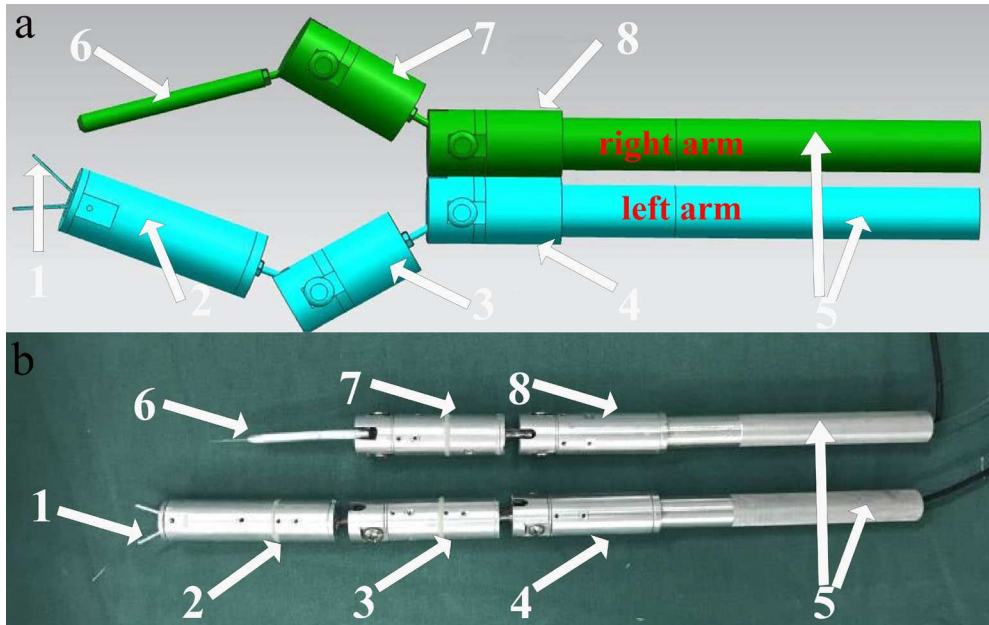
309 **Conclusion:** This bimanual surgical robot has the potential to become a surgical
310 instrument for simple intraperitoneal surgery. It can provide a small, portable and
311 inexpensive surgical robot system.

312 **Methods:**

313 **Mechanical design:**

314 The bimanual robot consists of two arms (Fig.7). The left arm consists of three
315 motor units, two revolute joints and grippers. The right arm contains two revolute joints,
316 two motor units and a laser fiber port. Shoulder actuation units can form the shoulder
317 triangle by moving the elbow actuation unit range 0 to 90 degrees. Elbow actuation
318 units can form the elbow triangle by moving the gripper actuation unit or laser head
319 range from 0 to 90 degrees. The diameter of left and right arms is 14mm, the length is
320 330mm, and the weight of one arm is about 200g. The bimanual robot can be inserted
321 into the abdominal cavity in a columnar constriction (Fig.1b) through a traditional
322 laparoscopic port. In order to meet the requirements of forming an operation triangle

323 during operation, the robot can unfold a shoulder-elbow shape when arriving at the
324 work area.

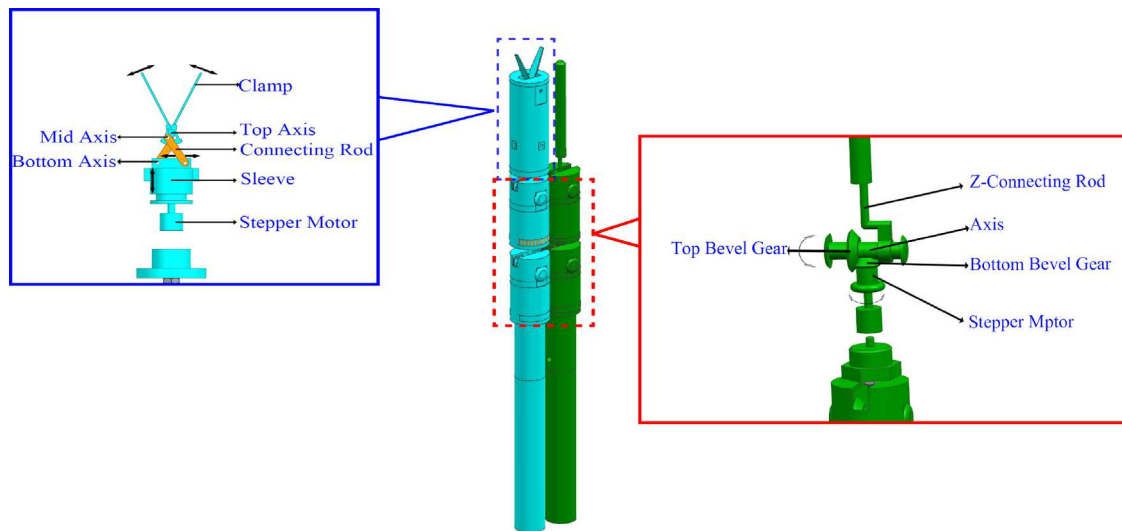


325 Fig.7 bimanual robot. (1=gripper, 2= gripper actuation unit,3= elbow actuation
326 unit(left),4= shoulder actuation unit(left),5= Handheld part,6= laser fiber port,7= laser
327 head actuation unit/elbow actuation unit(right),8= shoulder actuation unit(right))

328 **Internal structure:**

329 The internal structure of shoulder actuation unit and elbow actuation unit of left arm is
330 same as the right arm (Fig.8). Those actuation unit driving force is provided by stepper
331 motor. The motor that drives the rotation of the bottom bevel gear and top bevel gear,
332 then driving the swing of the next part through the axis by the Z-connecting rod. Gripper
333 actuation unit also use stepper motor to supply power, the motor and sleeve is connected
334 by threaded. So, sleeve can move up and down when the motor rotating and inversion.
335 In addition, as the sleeve moving, the connecting rod is pulled through the lower and
336 middle axis to move, which causes the gripper to create a grasping and opening motion

337 around the top axis.



338

339

Fig.8 internal structure of bimanual robot

340 **Data processing:**

341 The workspaces of the bimanual robot were analyzed by MATLAB R2019a, kinematic
342 simulation analysis and Modal analysis were analyzed by NX 12.0.

343 **Supplementary information:**

344 **Acknowledgements:**

345 The authors thank Dongguan Zhongshi Hardware Co. LTD for support during
346 processing robot.

347 **Authors' contributions:**

348 Each author is expected to have made substantial contributions to the conception and
349 design of the work. ZF, DHD, YW, TM completed the vitro experiment, ZF have
350 drafted the manuscript, HYZ and YL contributed to the drafting and revision. DHD and
351 HC essentially contributed to the data acquisition, processing and analysis. All authors
352 read and approved the final manuscript.

353 **Funding:**

354 This project received funding from the Science and Technology Innovation Project of
355 Shaanxi Province (No. 2016KTZDGY06-05-01).

356 **Ethics approval and consent to participate:**

357 Not applicable. There is no clinical trial or animals experiment.

358 **Consent for publication:**

359 Not applicable. There is no volunteer.

360 **Availability of data and materials:**

361 All data generated or analyzed during this study are included in this published article.

362 **Competing interests:**

363 The authors declare that they have no competing financial interests or personal
364 relationships that could have appeared to influence the work reported in this paper;

365 **References:**

- 366 1. Hewett PJ, Allardyce RA, Bagshaw PF, Frampton CM, Frizelle FA, Rieger NA, et al. Short-term
367 outcomes of the Australasian randomized clinical study comparing laparoscopic and conventional
368 open surgical treatments for colon cancer: the ALCCaS trial. *Ann Surg.* 2008;248(5):728-38.
- 369 2. Guillou PJ, Quirke P, Thorpe H, Walker J, Jayne DG, Smith AM, et al. Short-term endpoints of
370 conventional versus laparoscopic-assisted surgery in patients with colorectal cancer (MRC
371 CLASICC trial): multicentre, randomised controlled trial. *Lancet.* 2005;365(9472):1718-26.
- 372 3. Braga M, Vignali A, Gianotti L, Zuliani W, Radaelli G, Gruarin P, et al. Laparoscopic versus open
373 colorectal surgery: a randomized trial on short-term outcome. *Ann Surg.* 2002;236(6):759-66;
374 discussion 67.
- 375 4. Veldkamp R, Kuhry E, Hop WC, Jeekel J, Kazemier G, Bonjer HJ, et al. Laparoscopic surgery

376 versus open surgery for colon cancer: short-term outcomes of a randomised trial. *Lancet Oncol.*
377 2005;6(7):477-84.

378 5. Fleshman J, Sargent DJ, Green E, Anvari M, Stryker SJ, Beart RW, Jr., et al. Laparoscopic
379 colectomy for cancer is not inferior to open surgery based on 5-year data from the COST Study
380 Group trial. *Ann Surg.* 2007;246(4):655-62; discussion 62-4.

381 6. Pelosi MA, Pelosi MA, 3rd. Laparoscopic supracervical hysterectomy using a single-umbilical
382 puncture (mini-laparoscopy). *J Reprod Med.* 1992;37(9):777-84.

383 7. Tei M, Wakasugi M, Omori T, Ueshima S, Tori M, Akamatsu H. Single-port laparoscopic
384 colectomy is safe and feasible in patients with previous abdominal surgery. *Am J Surg.*
385 2015;209(6):1007-12.

386 8. Ateş O, Havgüder G, Olguner M, Akgür FM. Single-port laparoscopic appendectomy
387 conducted intracorporeally with the aid of a transabdominal sling suture. *Journal of Pediatric*
388 *Surgery.* 2007;42(6):1071-4.

389 9. Podolsky ER, Rottman SJ, Poblete H, King SA, Curcillo PG. Single port access (SPA)
390 cholecystectomy: a completely transumbilical approach. *J Laparoendosc Adv Surg Tech A.*
391 2009;19(2):219-22.

392 10. Daher R, Chouillard E, Panis Y. New trends in colorectal surgery: single port and natural orifice
393 techniques. *World J Gastroenterol.* 2014;20(48):18104-20.

394 11. Kim SJ, Choi BJ, Lee SC. Overview of single-port laparoscopic surgery for colorectal cancers:
395 past, present, and the future. *World J Gastroenterol.* 2014;20(4):997-1004.

396 12. Leal Ghezzi T, Campos Corleta O. 30 Years of Robotic Surgery. *World J Surg.*
397 2016;40(10):2550-7.

- 398 13. Agarwal DK, Sharma V, Toussi A, Viers BR, Tollefson MK, Gettman MT, et al. Initial Experience
399 with da Vinci Single-port Robot-assisted Radical Prostatectomies. (1873-7560 (Electronic)).
- 400 14. Haber GP, Autorino R Fau - Laydner H, Laydner H Fau - Yang B, Yang B Fau - White MA,
401 White Ma Fau - Hillyer S, Hillyer S Fau - Altunrende F, et al. SPIDER surgical system for urologic
402 procedures with laparoendoscopic single-site surgery: from initial laboratory experience to first
403 clinical application. (1873-7560 (Electronic)).
- 404 15. Allemann P, Leroy J, Asakuma M, Al Abeidi F, Dallemagne B, Marescaux J. Robotics May
405 Overcome Technical Limitations of Single-Trocar Surgery: An Experimental Prospective Study of
406 Nissen Fundoplication. *Archives of Surgery*. 2010;145(3):267-71.
- 407 16. Dobbs RA-O, Halgrimson WR, Madueke I, Vigneswaran HT, Wilson JO, Crivellaro S. Single-
408 port robot-assisted laparoscopic radical prostatectomy: initial experience and technique with the
409 da Vinci(®) SP platform. (1464-410X (Electronic)).
- 410 17. Kaouk J, Garisto JA-O, Eltemamy M, Bertolo RA-O. Step-by-step technique for single-port
411 robot-assisted radical cystectomy and pelvic lymph nodes dissection using the da Vinci(®) SP™
412 surgical system. LID - 10.1111/bju.14744 [doi]. (1464-410X (Electronic)).
- 413 18. Park SY, Kim HK, Jang DS, Han KN, Kim DJ. Initial Experiences With Robotic Single-Site
414 Thoracic Surgery for Mediastinal Masses. *Ann Thorac Surg*. 2019;107(1):242-7.
- 415 19. Park YM, Kim DH, Kang MS, Lim JY, Choi EC, Koh YW, et al. The First Human Trial of Transoral
416 Robotic Surgery Using a Single-Port Robotic System in the Treatment of Laryngo-Pharyngeal
417 Cancer. *Ann Surg Oncol*. 2019;26(13):4472-80.
- 418 20. Holsinger FC. A flexible, single-arm robotic surgical system for transoral resection of the tonsil
419 and lateral pharyngeal wall: Next-generation robotic head and neck surgery. *Laryngoscope*.

420 2016;126(4):864-9.

421 21. Bhayani SB, Link RE, Varkarakis JM, Kavoussi LR. Complete daVinci versus laparoscopic
422 pyeloplasty: cost analysis. *J Endourol.* 2005;19(3):327-32.

423 22. Fong ZV, Wolf AM, Doria C, Berger AC, Rosato EL, Palazzo F. Hemorrhagic hepatic cyst: report
424 of a case and review of the literature with emphasis on clinical approach and management. *J*
425 *Gastrointest Surg.* 2012;16(9):1782-9.

426 23. Kaneya Y, Yoshida H, Matsutani T, Hirakata A, Matsushita A, Suzuki S, et al. Biliary obstruction
427 due to a huge simple hepatic cyst treated with laparoscopic resection. *J Nippon Med Sch.*
428 2011;78(2):105-9.

429 24. Klingler PJ, Gadenstätter M, Schmid T, Bodner E, Schwelberger HG. Treatment of hepatic cysts
430 in the era of laparoscopic surgery. *Br J Surg.* 1997;84(4):438-44.

431 25. Ma T, Chai YC, Zhu HY, Chen H, Wang Y, Li QS, et al. Effects of Different 980-nm Diode Laser
432 Parameters in Hepatectomy. *Lasers Surg Med.* 2019;51(8):720-6.

433 26. Dong DH, Zhu HY, Luo Y, Zhang HK, Xiang JX, Xue F, et al. Miniature magnetically anchored
434 and controlled camera system for trocar-less laparoscopy. *World J Gastroenterol.*
435 2017;23(12):2168-74.

436 27. Ph M. From the first laparoscopic cholecystectomy to the frontiers of laparoscopic surgery:
437 The futures prospectives. *Dig Surg.* 1991(8):124-5.

438 28. Monson JR. Advanced techniques in abdominal surgery. *BMJ.* 1993;307(6915):1346-50.

439 29. Rutherford JC, Stowasser M, Tunny TJ, Klemm SA, Gordon RD. Laparoscopic adrenalectomy.
440 *World J Surg.* 1996;20(7):758-60; discussion 61.

441 30. Nelson H, Sargent DJ, Wieand HS, Fleshman J, Anvari M, Stryker SJ, et al. A comparison of

442 laparoscopically assisted and open colectomy for colon cancer. *N Engl J Med.* 2004;350(20):2050-
443 9.

444 31. Phillips EH, Franklin M, Carroll BJ, Fallas MJ, Ramos R, Rosenthal D. Laparoscopic colectomy.
445 *Ann Surg.* 1992;216(6):703-7.

446 32. Bucher P, Pugin F Fau - Buchs NC, Buchs Nc Fau - Ostermann S, Ostermann S Fau - Morel P,
447 Morel P. Randomized clinical trial of laparoendoscopic single-site versus conventional
448 laparoscopic cholecystectomy. *British Journal of Surgery.* 2011;98(1365-2168 (Electronic)):1695-
449 702.

450 33. Tsimoyiannis EC, Tsimogiannis KE, Pappas-Gogos G, Farantos C, Benetatos N, Mavridou P, et
451 al. Different pain scores in single transumbilical incision laparoscopic cholecystectomy versus
452 classic laparoscopic cholecystectomy: a randomized controlled trial. *Surg Endosc.*
453 2010;24(8):1842-8.

454 34. Wang Y-B, Xia J, Zhang J-Y, Gong J-P, Wang X-M. Effectiveness and safety of single-port
455 versus multi-port laparoscopic surgery for treating liver diseases: a meta-analysis. *Surgical*
456 *Endoscopy.* 2016;31(4):1524-37.

457 35. Krenzien F, Pratschke J, Zorron R. Assessment of Intra-gastric Single-Port Surgery for Gastric
458 Tumors. *JAMA Surg.* 2017;152(8):793-4.

459 36. Costedio MM, Remzi FH. Single-port laparoscopic colectomy. *Tech Coloproctol*
460 2013;17(1):29-34.

461 37. Aly OE, Black DH, Rehman H, Ahmed I. Single incision laparoscopic appendectomy versus
462 conventional three-port laparoscopic appendectomy: A systematic review and meta-analysis. *Int*
463 *J Surg.* 2016;35:120-8.

- 464 38. Leroy J, Cahill Ra Fau - Peretta S, Peretta S Fau - Marescaux J, Marescaux J. Single port
465 sigmoidectomy in an experimental model with survival. (1553-3506 (Print)).
- 466 39. Tracy CR, Raman Jd Fau - Cadeddu JA, Cadeddu Ja Fau - Rane A, Rane A. Laparoendoscopic
467 single-site surgery in urology: where have we been and where are we heading? (1743-4289
468 (Electronic)).
- 469 40. Lee H, Cheon B, Hwang M, Kang D, Kwon D-S. A master manipulator with a remote-center-
470 of-motion kinematic structure for a minimally invasive robotic surgical system. International
471 Journal of Medical Robotics and Computer Assisted Surgery. 2018;14(1).
- 472 41. Pietrabissa A, Pugliese L, Vinci A, Peri A, Tinozzi FP, Cavazzi E, et al. Short-term outcomes of
473 single-site robotic cholecystectomy versus four-port laparoscopic cholecystectomy: a prospective,
474 randomized, double-blind trial. Surg Endosc. 2016;30(7):3089-97.
- 475 42. Spinoglio G, Lenti LM, Maglione V, Lucido FS, Priora F, Bianchi PP, et al. Single-site robotic
476 cholecystectomy (SSRC) versus single-incision laparoscopic cholecystectomy (SILC): comparison
477 of learning curves. First European experience. Surg Endosc. 2012;26(6):1648-55.
- 478 43. Cruz CJ, Yang HY, Kang I, Kang CM, Lee WJ. Technical feasibility of da Vinci SP single-port
479 robotic cholecystectomy: a case report. Ann Surg Treat Res. 2019;97(4):217-21.
- 480 44. Isaac-Lowry OJ, Okamoto S, Pedram SA, Woo R, Berkelman P. Compact teleoperated
481 laparoendoscopic single-site robotic surgical system: Kinematics, control, and operation.
482 International Journal of Medical Robotics and Computer Assisted Surgery. 2017;13(4).
- 483 45. Li J, Li X, Wang J, Xing Y, Wang S, Ren X. Design and evaluation of a variable stiffness manual
484 operating platform for laparoendoscopic single site surgery (LESS). International Journal of
485 Medical Robotics and Computer Assisted Surgery. 2017;13(4).

- 486 46. Schneider B, Jr., Abatti PJ. Electrical characteristics of the sparks produced by electrosurgical
487 devices. IEEE Trans Biomed Eng. 2008;55(2 Pt 1):589-93.
- 488 47. Hwang M, Yang UJ, Kong D, Chung DG, Lim JG, Lee DH, et al. A single port surgical robot
489 system with novel elbow joint mechanism for high force transmission. Int J Med Robot. 2017;13(4).
- 490

Figures

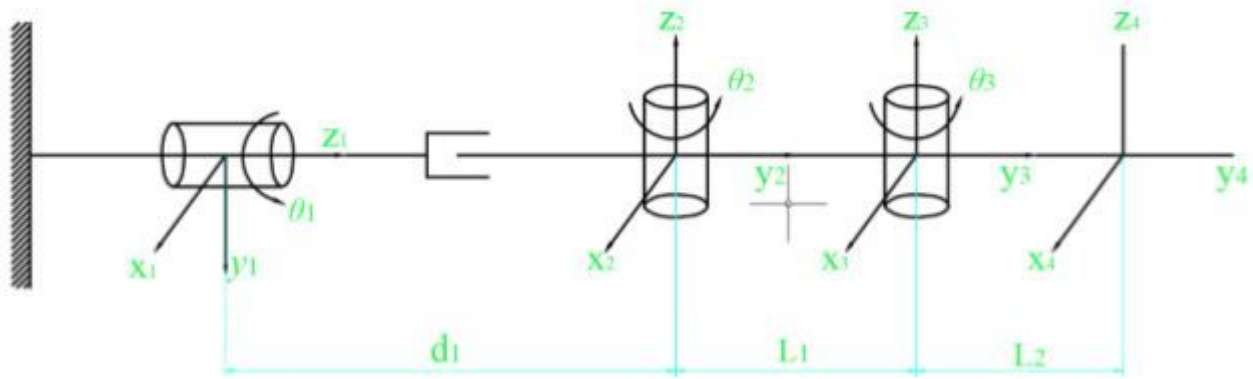


Figure 1

Coordinate system of each link of the robot

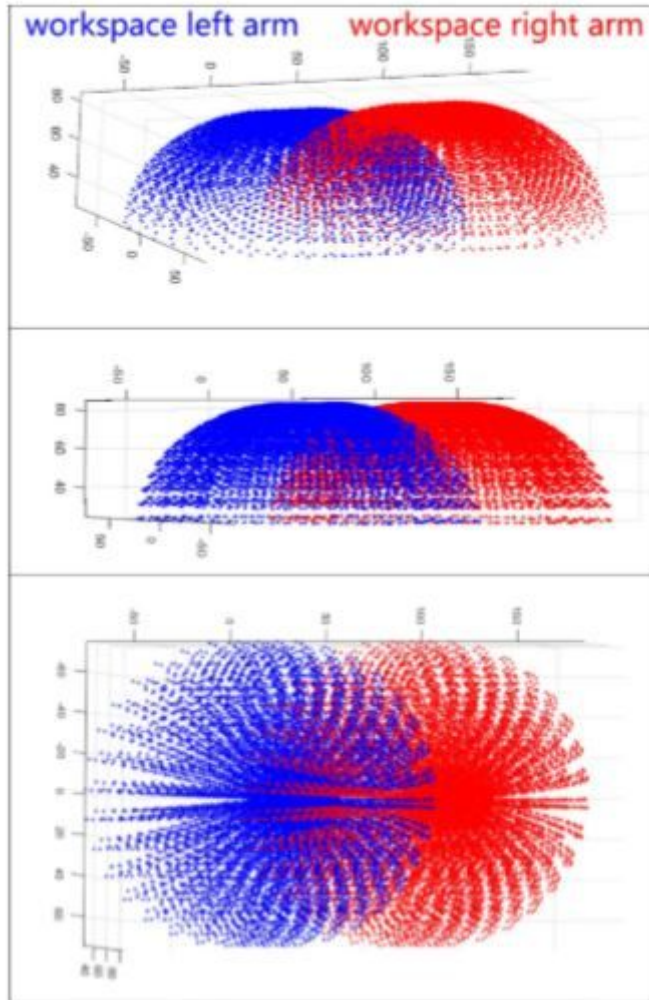


Figure 2

The workspaces of the bimanual robot

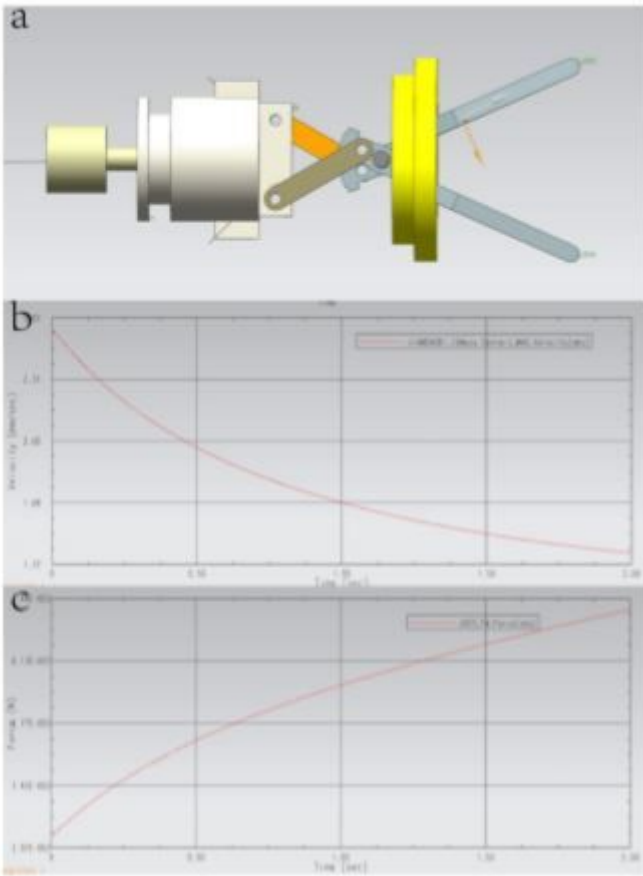


Figure 3

kinematic simulation analysis

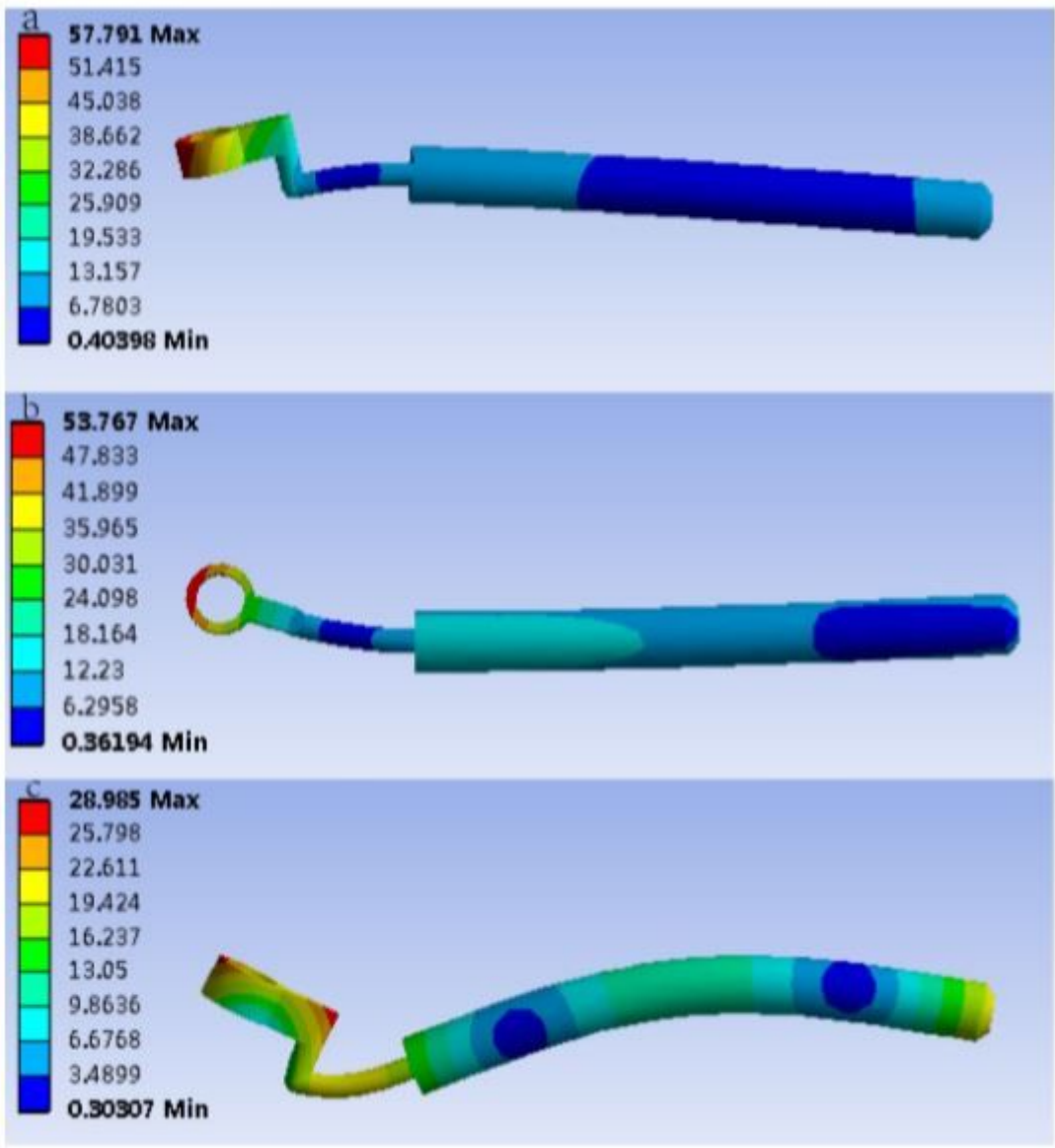


Figure 4

odal analysis of the left arm; a: first-order modal frequencies of the left bimanual robot; b. second-order modal frequencies of the left bimanual robot; c: third-order modal frequencies of the left bimanual robot

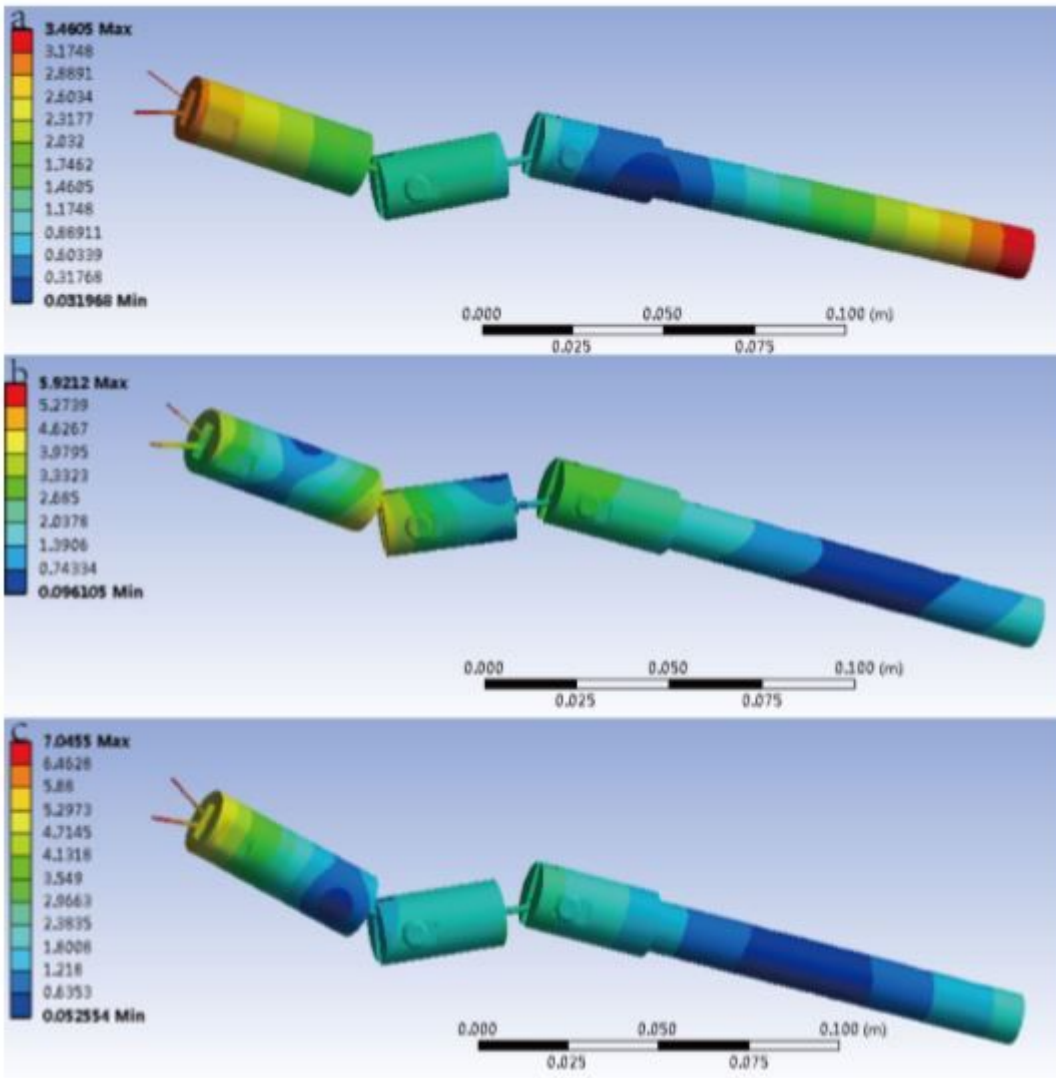


Figure 5

a: first-order modal frequencies of the laser head; b: second-order modal frequencies of the laser head; c: third-order modal frequencies of the laser head

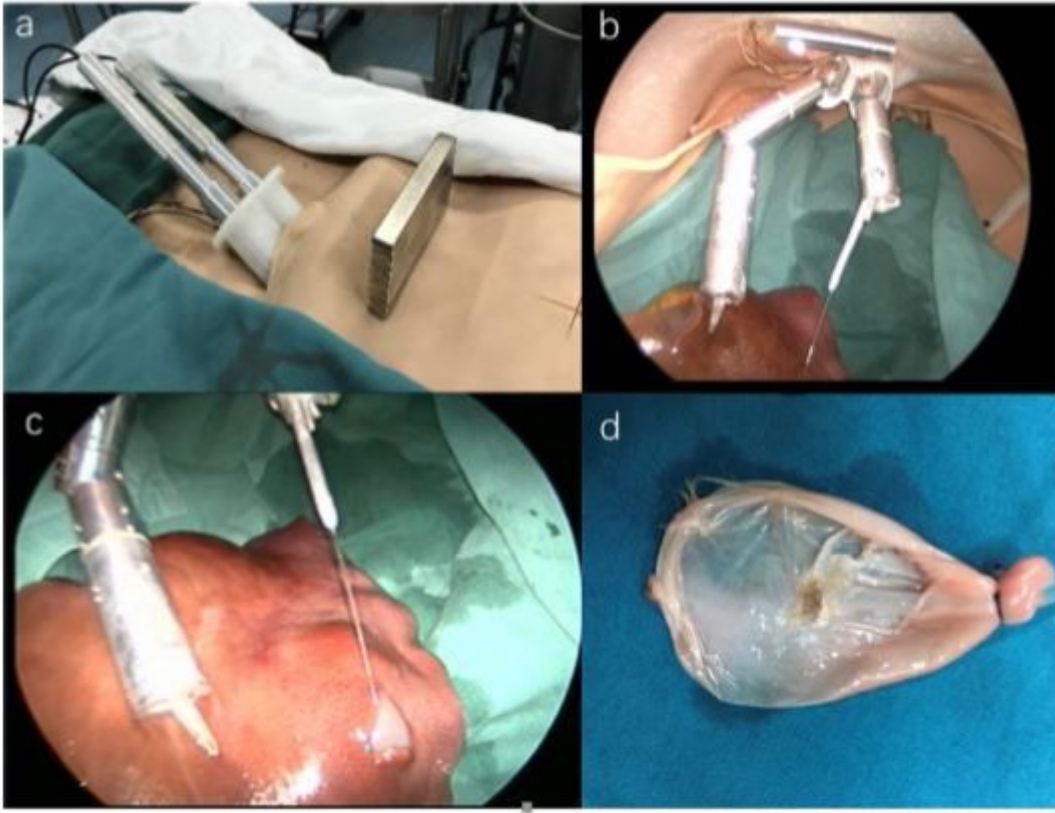


Figure 6

vitro experiment of fenestration and drainage of hepatic cyst

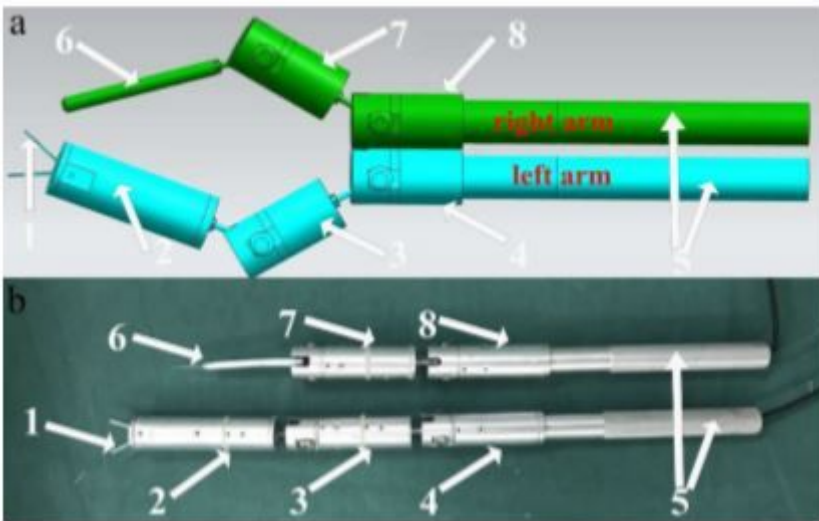


Figure 7

bimanual robot. (1=grripper, 2= gripper actuation unit,3= elbow actuation unit(left),4= shoulder actuation unit(left),5= Handheld part,6= laser fiber port,7= laser head actuation unit/elbow actuation unit(right),8= shoulder actuation unit(right))

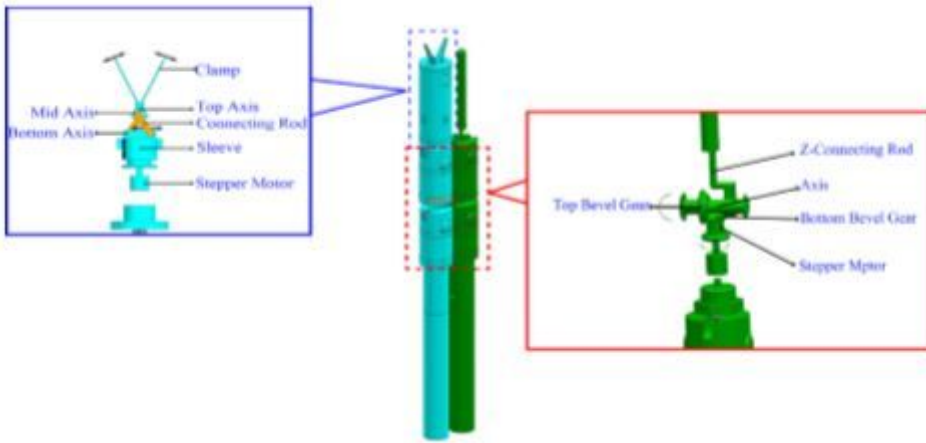


Figure 8

internal structure of bimanual robot